

THEORETICAL PROCEDURE TO PREDICT THE LOCAL BUCKLING RESISTANCE OF ALUMINIUM MEMBERS IN ELASTIC-PLASTIC RANGE

VINCENZO PILUSO¹, ALESSANDRO PISAPIA¹

¹ University of Salerno
Via Giovanni Paolo II, 132-84084 Fisciano (SA), Italy
v.piluso@unisa.it, alpisapia@unisa.it

KEY WORDS: Local buckling, Deformation theory of plasticity, aluminium alloys

ABSTRACT

In the present research work, a theoretical approach to evaluate the ultimate resistance of aluminium alloy members subjected to local buckling under uniform compression is provided. In particular, starting from the J_2 deformation theory of plasticity, the theory of plastic buckling of plates has been extended including the variability of the Poisson's ratio depending on the stress levels. The differential equation of the plates at the onset of buckling is developed and the corresponding solution is determined. This derivation represents an innovative step compared to the theoretical solutions currently existing in the technical literature because the variability of the Poisson's ratio in the elastic-plastic region is commonly not accounted.

Subsequently, starting from the obtained closed-form solution, the interactive buckling either in the elastic or in the plastic range of a generic aluminium members in compression is analysed. Two types of cross-sections are analysed: box-shaped members. To this scope, the Levy solution of the differential equation of a single plate in elastic-plastic range is applied to the assembled plates constituting the cross-sections.

Obviously, the interaction between the plate elements constituting the section is explicitly accounted by means of the boundary conditions accounting for restraining action. The previous boundary conditions lead to a system of equations whose trivial solution corresponds to the member in its non-deformed configuration. The prediction of the critical stress corresponding to local buckling in the elastic-plastic region is obtained as the value corresponding to the existence of a non-trivial solution for which the determinant of the matrix of the equation system is equal to zero. Finally, in order to consider the geometric imperfections of aluminium members, the procedure has been repeated by considering different geometric properties of plates composing the analysed cross-sections.

1. INTRODUCTION

The ultimate behaviour of aluminium members under uniform compression or in bending is strongly affected by the local buckling effects, the strain hardening behaviour and the interaction between the plate composing the cross-sections. The current provision, EN199-1-1[1], adopts the same approach used for the carbon steel members. However, it is recognized that this approach is very conservative in the case of aluminium alloys[2]-[6]. Consequently,

some simplified approaches are presented in the scientific literature as the continuous strength method (CSM), direct strength method (DSM) or the extension of effective thickness method (ETM)[7]-[9]. In this work an alternative theoretical procedure has been developed starting from the deformation theory of plasticity.

It is well known that the occurrence of buckling leads to a sudden loss of strength due to second-order effects rising from the deformed configuration resulting from buckling itself. In the case of metal structures, depending on the overall slenderness and on the local slenderness of the structural elements, buckling can be of concern for the structure as a whole, the individual structural elements or the plate elements constituting the member section. Besides, it can occur either in the elastic or in the plastic range. So, the first problem to deal with the theoretical study of the elastic-plastic response of structures under certain loading conditions is the definition of appropriate stress-strain relationships to describe the mechanical behaviour of material. In the simple cases of pure compression or tension, it is possible to adopt uniaxial stress-strain curves, however, under actual loading conditions, particular attention must be devoted to the material behaviour under multiaxial stress states. Generally, the plasticity models currently adopted for metal structures can be divided into two main groups: 1) the flow (Lévy-Mises) theory of plasticity, 2) the deformation (Hencky-Nadai) theory of plasticity. the flow theory of plasticity leads to a path-dependent relationship where the current strain depends not only on the value of the current total stress but also on how the actual stress value has been reached. Conversely, the deformation theory of plasticity represents essentially a special path-independent nonlinear constitutive law. Although from the scientific point of view, the flow theory of plasticity is more rigorous than second one, in many engineering problems regarding the inelastic buckling of structures, the deformation theory seems to be more in agreement with the experimental results. This phenomenon is usually referred to as the “plastic buckling paradox” [10]-[12].

This work is not aimed to contribute to solving the controversies resulting from the plastic buckling paradox. The theoretical study herein presented will refer to the deformation theory of plasticity. The novelty of this work regards the introduction of the variability of the Poisson’s ratio in the elastic-plastic range, i.e., as dependent on the stress intensity measure, in the evaluation of the plate buckling differential equation. Then, the elastic-plastic plate buckling differential equation is used to define a theoretical procedure to estimate the ultimate resistance of aluminium members subjected to local buckling in compression.

2. PLATE BUCKLING EQUATION IN ELASTIC-PLASTIC RANGE

In this section, the plate buckling equation in elastoplastic region is provided. In particular, starting from the unified theory of plastic buckling presented by Stowell et al. [13], the general differential equation of plate stability has been derived in the elastic-plastic range to account for the mechanical non-linearity of aluminium material. The difference between the equation provided by Stowell and the one herein presented regards the assumption of the Poisson’s ratio. In fact, according to the classical Stowell’s and Ilyushin’s [14] assumption, the Poisson’s ratio is assumed equal to 0.50 according to the plastically incompressible state. Conversely, in the theoretical developments the Poisson’s ratio is assumed to be dependent on the stress level as suggested by Gerard and Wildhorn [15]. Consequently, the variation of stresses during buckling are derived according to the procedure outlined by Jones [16].

The mathematical steps to derive the stability equation of a single plate in the elastic-plastic region are provided in the following sections.

2.1. Relations in J_2 Deformation Theory of Plasticity

According to the J_2 deformation theory of plasticity for isotropic materials under biaxial plane stress state ($\sigma_z = \tau_{xz} = \tau_{yz} = 0$), the stress intensity and the corresponding strain intensity are given by:

$$\sigma_i = \sqrt{\sigma_x^2 + \sigma_y^2 - \sigma_x \sigma_y + 3\tau_{xy}^2} \quad (1)$$

and:

$$\varepsilon_i = \frac{1}{1-\nu^2} \sqrt{(1-\nu+\nu^2)(\varepsilon_x^2 + \varepsilon_y^2) - (1-4\nu+\nu^2)\varepsilon_x \varepsilon_y + \frac{3}{4}(1-\nu)^2 \gamma_{xy}^2} \quad (2)$$

While the stress-strain relations with general non-linear material properties are equal to:

$$\sigma_x = \frac{E_s}{1-\nu^2} (\varepsilon_x + \nu \varepsilon_y) \quad \sigma_y = \frac{E_s}{1-\nu^2} (\varepsilon_y + \nu \varepsilon_x) \quad \tau_{xy} = \frac{E_s}{2(1+\nu)} \gamma_{xy} \quad (3)$$

where E_s represents the secant modulus and it is given by:

$$E_s = \frac{\sigma_i}{\varepsilon_i} \quad (4)$$

The coefficient ν is the Poisson's ratio and, in the elastic plastic region, his expression is provided by Gerard and Wildhorn [15]:

$$\nu = \nu_p - (\nu_p - \nu_e) \frac{E_s}{E} \quad (5)$$

where ν_e and ν_p are, respectively, the Poisson's ratio in elastic and plastic range. By rearranging Eq. (3), it is possible to express the strains as function of the stresses:

$$\varepsilon_x = \frac{\sigma_x - \nu \sigma_y}{E_s} \quad \varepsilon_y = \frac{\sigma_y - \nu \sigma_x}{E_s} \quad \gamma_{xy} = \frac{2(1+\nu)}{E_s} \tau_{xy} \quad (6)$$

2.2. Variation of Stresses during Buckling

According to Figure 1, the stresses during buckling vary from their pre-buckling values. By considering the variability of E_s and ν with the stress levels, the variation of the normal stress $\delta\sigma_x$ can be derived from the first of Eqns. (3) as follows:

$$\delta\sigma_x = \frac{E_s}{1-\nu^2} [\delta\varepsilon_x + \nu\delta\varepsilon_y] + \frac{\delta E_s}{1-\nu^2} (\varepsilon_x + \nu\varepsilon_y) + E_s \varepsilon_x \delta \left[\frac{1}{1-\nu^2} \right] + E_s \varepsilon_y \delta \left[\frac{\nu}{1-\nu^2} \right] \quad (7)$$

it is worthwhile noting that:

$$\delta E_s = -\frac{E_s^2}{\sigma_i} \left(1 - \frac{E_t}{E_s}\right) \delta\varepsilon_i \quad \delta \left[\frac{1}{1-\nu^2} \right] = \frac{2\nu}{(1-\nu^2)^2} \delta\nu \quad \left[\frac{\nu}{1-\nu^2} \right] = \frac{1+\nu^2}{(1-\nu^2)^2} \delta\nu \quad (8)$$

where the variation of Poisson's ratio is equal to:

$$\delta\nu = \left(\frac{1/2 - \nu_e}{E} \right) \left(1 - \frac{E_t}{E_s}\right) \frac{E_s^2}{\sigma_i} \delta\varepsilon_i \quad (9)$$

where E_t represents the tangent modulus. By substituting Eqns. (8) and (9) into Eq.(7), and taking into account the Eq.(3), it is obtained:

$$\delta\sigma_x = \frac{E_s}{1-\nu^2} (\delta\varepsilon_x + \nu\delta\varepsilon_y) - \frac{E_s}{\sigma_i} \left(1 - \frac{E_t}{E_s}\right) \left[\sigma_x - \frac{1-2\nu}{2(1-\nu^2)} (\sigma_y + \nu\sigma_x) \right] \delta\varepsilon_i \quad (10)$$

According to the mathematical steps reported in [17] and [18], the variation of the strain intensity has to be expressed as a function of the stress levels and the variation of the strains as follows:

$$\delta\varepsilon_i = \frac{1}{2H\sigma_i(1-\nu^2)} \{ [(2-\nu)\sigma_x - (1-2\nu)\sigma_y]\delta\varepsilon_x + [(2-\nu)\sigma_y - (1-2\nu)\sigma_x]\delta\varepsilon_y + [3(1-\nu)\tau_{xy}]\delta\gamma_{xy} \} \quad (11)$$

where H is equal to:

$$H = 1 - \frac{1-2\nu}{2(1-\nu^2)} \left(1 - \frac{E_t}{E_s} \right) \left\{ 2\nu + \frac{1}{2\sigma_i^2} [2(\nu+2)\sigma_x\sigma_y - (2\nu+1)(\sigma_x^2 + \sigma_y^2) - 6(1+\nu)\tau_{xy}^2] \right\} \quad (12)$$

By substituting Eq.(11) into Eq.(10), the stress variation is expressed as a function of the stress levels and strain variations:

$$\delta\sigma_x = \frac{E_s}{1-\nu^2} \left\{ (\delta\varepsilon_x + \nu\delta\varepsilon_y) + \Phi_x \left[k_x\sigma_x\delta\varepsilon_x + k_y\sigma_y\delta\varepsilon_y + \frac{1}{2}k_{xy}\tau_{xy}\delta\gamma_{xy} \right] \right\} \quad (13)$$

where:

$$\begin{aligned} \Phi_x &= \frac{1}{2H\sigma_i^2} \left(1 - \frac{E_t}{E_s} \right) \left[\frac{1-2\nu}{2(1-\nu^2)} (\sigma_y + \nu\sigma_x) - \sigma_x \right] \\ k_x &= [(2-\nu) - (1-2\nu)\sigma_y/\sigma_x] \\ k_y &= [(2-\nu) - (1-2\nu)\sigma_x/\sigma_y] \\ k_{xy} &= 6(1-\nu) \end{aligned} \quad (14)$$

By exchanging x with y , the stress variation $\delta\sigma_y$ is equal to:

$$\delta\sigma_y = \frac{E_s}{1-\nu^2} \left\{ (\delta\varepsilon_y + \nu\delta\varepsilon_x) + \Phi_y \left[k_x\sigma_x\delta\varepsilon_x + k_y\sigma_y\delta\varepsilon_y + \frac{1}{2}k_{xy}\tau_{xy}\delta\gamma_{xy} \right] \right\} \quad (15)$$

where Φ_y is equal to:

$$\Phi_y = \frac{1}{2H\sigma_i^2} \left(1 - \frac{E_t}{E_s} \right) \left[\frac{1-2\nu}{2(1-\nu^2)} (\sigma_x + \nu\sigma_y) - \sigma_y \right] \quad (16)$$

From Eqns. (3) (third):

$$\delta\tau_{xy} = \frac{E_s}{2(1+\nu)} \delta\gamma_{xy} + \gamma_{xy} \left[\frac{\delta E_s}{2(1+\nu)} + \frac{E_s}{2} \frac{\delta\nu}{(1+\nu)^2} \right] \quad (17)$$

Accounting for Eqns. (8) and (9), the variation of the shear stress is given by:

$$\delta\tau_{xy} = \frac{E_s}{2(1-\nu^2)} \left\{ (1-\nu)\delta\gamma_{xy} - \frac{1}{2\sigma_i} \left(1 - \frac{E_t}{E_s} \right) 6(1-\nu)\tau_{xy}\delta\varepsilon_i \right\} \quad (18)$$

Finally, by substituting Eq.(11) into Eq.(18), also the variation of the shear stress is expressed as a function of the stress levels and strain variations:

$$\delta\tau_{xy} = \frac{E_s}{2(1-\nu^2)} \left\{ (1-\nu)\delta\gamma_{xy} + \Phi_{xy} \left[k_x\sigma_x\delta\varepsilon_x + k_y\sigma_y\delta\varepsilon_y + \frac{1}{2}k_{xy}\tau_{xy}\delta\gamma_{xy} \right] \right\} \quad (19)$$

where Φ_{xy} is equal to:

$$\Phi_{xy} = -\frac{3}{2H\sigma_i^2} \left(1 - \frac{E_t}{E_s} \right) \left(\frac{\tau_{xy}}{1+\nu} \right) \quad (20)$$

2.3. Variation of internal actions in thin plates

According to the theory of thin plates, it is possible to assume that the segments which are orthogonal to the mid-plane of the plate remain orthogonal also in the deformed configuration (Figure 2). Therefore, the strain variations are given by:

$$\delta\varepsilon_x = \delta\varepsilon_{x.0} - z\delta\chi_x \quad \delta\varepsilon_y = \delta\varepsilon_{y.0} - z\delta\chi_y \quad \delta\gamma_{xy} = 2\delta\varepsilon_{xy.0} - 2z\delta\chi_{xy} \quad (21)$$

where $\delta\varepsilon_{x.0}$, $\delta\varepsilon_{y.0}$ and $2\delta\varepsilon_{xy.0}$ are the strain variations at the mid-thickness line of the plate; $\delta\chi_x$, $\delta\chi_y$ and $2\delta\chi_{xy}$ are, respectively, the curvature variations and twisting, while z is the distance of the generic fibre from the mid-thickness line of the plate.

By substituting the previous relations into Eqns.(13),(15), (18) and by means of some mathematical steps, the following relationships are provided:

$$\begin{aligned}\delta\sigma_x &= \frac{E_s}{1-\nu^2} [(\delta\varepsilon_{x.0} + \nu\delta\varepsilon_{y.0}) - z(\delta\chi_x + \nu\delta\chi_y) - \Psi\sigma_x S_x^*(K_\varepsilon - zK_\chi)] \\ \delta\sigma_y &= \frac{E_s}{1-\nu^2} [(\delta\varepsilon_{y.0} + \nu\delta\varepsilon_{x.0}) - z(\delta\chi_y + \nu\delta\chi_x) - \Psi\sigma_y S_y^*(K_\varepsilon - zK_\chi)] \\ \delta\tau_{xy} &= \frac{E_s}{2(1-\nu^2)} [2(1-\nu)(\delta\varepsilon_{xy.0} - z\delta\chi_{xy}) - \Psi\tau_{xy} S_\tau^*(K_\varepsilon - zK_\chi)]\end{aligned}\quad (22)$$

where:

$$\begin{aligned}\Psi &= \frac{1}{2H\sigma_i^2} \left(1 - \frac{E_t}{E_s}\right) \\ S_x^* &= \left[1 - \frac{1-2\nu}{2(1-\nu^2)} \frac{(\sigma_y + \nu\sigma_x)}{\sigma_x}\right] = \frac{k_x}{2(1-\nu^2)} \\ S_y^* &= \left[1 - \frac{1-2\nu}{2(1-\nu^2)} \frac{(\sigma_x + \nu\sigma_y)}{\sigma_y}\right] = \frac{k_y}{2(1-\nu^2)} \\ S_\tau^* &= \frac{3}{1+\nu} \\ K_\varepsilon &= k_x\sigma_x\delta\varepsilon_{x.0} + k_y\sigma_y\delta\varepsilon_{y.0} + k_{xy}\tau_{xy}\delta\varepsilon_{xy.0} \\ K_\chi &= k_x\sigma_x\delta\chi_x + k_y\sigma_y\delta\chi_y + k_{xy}\tau_{xy}\delta\chi_{xy}\end{aligned}\quad (23)$$

The relationships reported in Eq.(22) represent the dependence between the stress variations on strain variations.

The variations of the bending and twisting moments due to buckling are given by:

$$\delta M_x = \int_{-t/2}^{+t/2} \delta\sigma_x \cdot z dz \quad \delta M_y = \int_{-t/2}^{+t/2} \delta\sigma_y \cdot z dz \quad \delta M_{xy} = \int_{-t/2}^{+t/2} \delta\tau_{xy} \cdot z dz \quad (24)$$

By substituting the relations presented in Eq.(23) into previous equation, it is obtained:

$$\begin{aligned}\delta M_x &= -D_s [A_{11}\delta\chi_x + A_{12}\delta\chi_y + A_{13}\delta\chi_{xy}] \\ \delta M_y &= -D_s [A_{21}\delta\chi_x + A_{22}\delta\chi_y + A_{23}\delta\chi_{xy}] \\ \delta M_{xy} &= -\frac{D_s}{2} [A_{31}\delta\chi_x + A_{32}\delta\chi_y + A_{33}\delta\chi_{xy}]\end{aligned}\quad (25)$$

where:

$$\begin{aligned}A_{11} &= 1 - \frac{\sigma_x^2}{2H\sigma_i^2} \left(1 - \frac{E_t}{E_s}\right) k_x S_x^* & A_{21} &= \nu - \frac{\sigma_x\sigma_y}{2H\sigma_i^2} \left(1 - \frac{E_t}{E_s}\right) k_x S_y^* \\ A_{12} &= \nu - \frac{\sigma_x\sigma_y}{2H\sigma_i^2} \left(1 - \frac{E_t}{E_s}\right) k_y S_x^* & A_{22} &= 1 - \frac{\sigma_y^2}{2H\sigma_i^2} \left(1 - \frac{E_t}{E_s}\right) k_y S_y^* \\ A_{13} &= -\frac{\sigma_x\tau_{xy}}{2H\sigma_i^2} \left(1 - \frac{E_t}{E_s}\right) k_{xy} S_x^* & A_{23} &= -\frac{\sigma_y\tau_{xy}}{2H\sigma_i^2} \left(1 - \frac{E_t}{E_s}\right) k_{xy} S_y^* \\ A_{31} &= -\frac{\sigma_x\tau_{xy}}{2H\sigma_i^2} \left(1 - \frac{E_t}{E_s}\right) k_x S_\tau^*\end{aligned}\quad (26)$$

$$A_{32} = -\frac{\sigma_y \tau_{xy}}{2H\sigma_i^2} \left(1 - \frac{E_t}{E_s}\right) k_y S_\tau^*$$

$$A_{33} = 2(1 - \nu) - \frac{\tau_{xy}^2}{2H\sigma_i^2} \left(1 - \frac{E_t}{E_s}\right) k_{xy} S_\tau^*$$

The symbol D_s represent the secant flexural stiffness of the plate and it is equal to:

$$D_s = \frac{E_s t^3}{12(1 - \nu^2)} \quad (27)$$

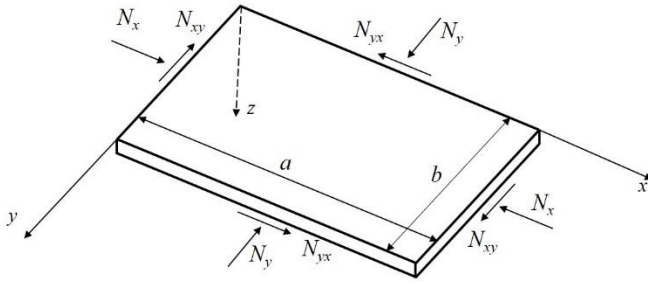


Figure 1. Single plate under membrane actions

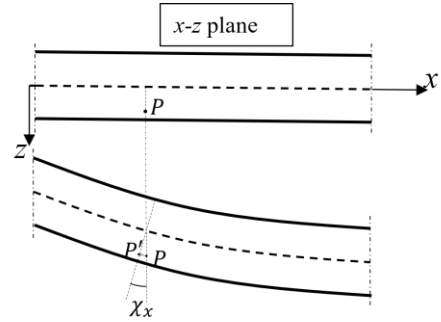


Figure 2. Orthogonality of section to mid-plane of plate

2.4. Equilibrium equation at the buckling

In the case of plate subjected to only membrane force, the bending deflection of the plate is equal to zero. Therefore, by denoting with $w = w(x, y)$ the bending deflection of the plate at buckling, the changes in curvatures are given by:

$$\delta\chi_x = \frac{\partial^2 w}{\partial x^2} \quad \delta\chi_y = \frac{\partial^2 w}{\partial y^2} \quad \delta\chi_{xy} = \frac{\partial^2 w}{\partial x \partial y} \quad (28)$$

Therefore, by denoting the membrane actions as N_x, N_y and N_{xy} , at the buckling, the differential equation of the plate under in-plane loading at buckling can be expressed as:

$$\frac{\partial^2(\delta M_x)}{\partial x^2} + 2\frac{\partial^2(\delta M_{xy})}{\partial x \partial y} + \frac{\partial^2(\delta M_y)}{\partial y^2} = N_x \frac{\partial^2 w}{\partial x^2} + 2N_{xy} \frac{\partial^2 w}{\partial x \partial y} + N_y \frac{\partial^2 w}{\partial y^2} \quad (29)$$

So, by substituting the relationships reported in Eqns.(25) and (28) into previous equation, the plate buckling differential equation accounting for the variability of the Poisson's ratio in the elastic-plastic range is provided:

$$C_1 \frac{\partial^4 w}{\partial x^4} - C_2 \frac{\partial^4 w}{\partial x^3 \partial y} + 2C_3 \frac{\partial^4 w}{\partial x^2 \partial y^2} - C_4 \frac{\partial^4 w}{\partial x \partial y^3} + C_5 \frac{\partial^4 w}{\partial y^4} = -\frac{1}{D_s} \left(N_x \frac{\partial^2 w}{\partial x^2} + 2N_{xy} \frac{\partial^2 w}{\partial x \partial y} + N_y \frac{\partial^2 w}{\partial y^2} \right) \quad (30)$$

where:

$$C_1 = A_{11} \quad C_2 = -(A_{13} + A_{31}) \quad C_3 = 0.5(A_{12} + A_{21} + A_{33}) \quad C_4 = -(A_{23} + A_{32}) \quad C_5 = A_{22} \quad (31)$$

Taking into account the Eqns.(14),(23) and (26), the final expressions of coefficients C_i are equal to:

$$C_1 = 1 - \frac{1}{4H\sigma_i^2(1 - \nu^2)} \left(1 - \frac{E_t}{E_s}\right) [(2 - \nu)\sigma_x - (1 - 2\nu)\sigma_y]^2$$

$$C_2 = \frac{3\tau_{xy}}{H\sigma_i^2(1 + \nu)} \left(1 - \frac{E_t}{E_s}\right) [(2 - \nu)\sigma_x - (1 - 2\nu)\sigma_y] \quad (32)$$

$$C_3 = 1 - \frac{1}{4H\sigma_i^2} \left(1 - \frac{E_t}{E_s}\right) \left\{ \frac{[(2-\nu)\sigma_x - (1-2\nu)\sigma_y][(2-\nu)\sigma_y - (1-2\nu)\sigma_x] + 18\tau_{xy}^2(1-\nu)^2}{1-\nu^2} \right\}$$

$$C_4 = \frac{3\tau_{xy}}{H\sigma_i^2(1+\nu)} \left(1 - \frac{E_t}{E_s}\right) [(2-\nu)\sigma_y - (1-2\nu)\sigma_x]$$

$$C_5 = 1 - \frac{1}{4H\sigma_i^2(1-\nu^2)} \left(1 - \frac{E_t}{E_s}\right) [(2-\nu)\sigma_y - (1-2\nu)\sigma_x]^2$$

It is easy to recognize that in the elastic range the value of coefficients C_1 , C_3 and C_5 is equal to 1.00 and the value of coefficients C_2 and C_4 is equal to zero because $E_t = E_s = E$. Consequently, Eq.(29) will provide the well-known *De Saint Venant* equation. Conversely, by imposing $\nu = \nu_p$, the mathematical relations of coefficients C_i are the same as those derived by Stowell[13].

2.5. Plate stability under uniform compression

The attention is focused on the analysis of box-shaped aluminium members under uniform compression. Consequently, according to Figure 3, the following reference is made to the case of plate uniaxial compression:

$$\sigma_x = \sigma_i \qquad \sigma_y = \tau_{xy} = 0 \qquad (33)$$

The differential equation, Eq.(30), is simplified as:

$$C_1 \frac{\partial^4 w}{\partial x^4} + 2C_3 \frac{\partial^4 w}{\partial x^2 \partial y^2} + C_5 \frac{\partial^4 w}{\partial y^4} = -\frac{N}{D_s} \frac{\partial^2 w}{\partial x^2} \qquad (34)$$

where the coefficients C_i are equal to:

$$C_1 = 1 - \frac{(2-\nu)^2}{4H(1-\nu^2)} \left(1 - \frac{E_t}{E_s}\right) \qquad C_5 = 1 - \frac{(1-2\nu)^2}{4H(1-\nu^2)} \left(1 - \frac{E_t}{E_s}\right)$$

$$C_3 = 1 + \frac{(2-\nu)(1-2\nu)}{4H(1-\nu^2)} \left(1 - \frac{E_t}{E_s}\right) \qquad H = 1 + \frac{(1-2\nu)^2}{4(1-\nu^2)} \left(1 - \frac{E_t}{E_s}\right) \qquad (35)$$

According to Levy's form, the solution of Eq.(34) can be found as:

$$w(x, y) = F(y) \sin\left(\frac{m\pi x}{a}\right) \qquad (36)$$

where a is the length of the plate and m is the number of half-waves along the longitudinal direction. By substituting Eq. (36) into Eq.(34), through some mathematical steps, the solution of the differential equation can be found as follows:

$$w(x, y) = (A_1 \cosh \alpha y + A_2 \sinh \alpha y + A_3 \cos \beta y + A_4 \sin \beta y) \sin kx \qquad (37)$$

where $k = m\pi/a$ and α, β are equal to:

$$\alpha = \sqrt{\frac{C_3 k^2}{C_5} + \sqrt{\left(\frac{C_3}{C_5}\right)^2 k^4 - k^2 \left(k^2 \frac{C_1}{C_5} - \frac{N}{D_s C_5}\right)}} \qquad \beta = \sqrt{-\frac{C_3 k^2}{C_5} + \sqrt{\left(\frac{C_3}{C_5}\right)^2 k^4 - k^2 \left(k^2 \frac{C_1}{C_5} - \frac{N}{D_s C_5}\right)}} \qquad (38)$$

The integration constants A_i have to be derived accounting for the boundary conditions. The writing of the boundary conditions can concern kinematic conditions (i.e. displacements and rotations) and static conditions (i.e. internal actions). Obviously, the trivial solution $\sin kx = 0$ has to be neglected.

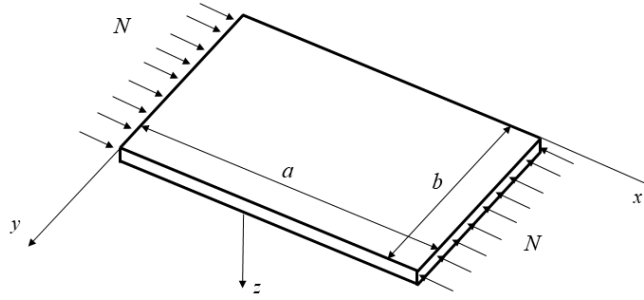


Figure 3. Single plate under uniform compression

3. APPLICATION OF THEORETIC PROCEDURE TO BOX SECTIONS

The theoretic procedure, reported in Section 2.5, can be applied to all plates constituting a generic aluminium cross-section. According to Figure 4, the application of procedure is reported with reference to the box-shaped aluminium member. So, Eq.(37) can be developed for plate 1 and plate 2 as follows:

$$\text{Plate 1: } w^{(1)}(x, y) = A_1^{(1)} \cosh \alpha y + A_2^{(1)} \sinh \alpha y + A_3^{(1)} \cos \beta y + A_4^{(1)} \sin \beta y \quad (39)$$

$$\text{Plate 2: } w^{(2)}(x, y) = A_1^{(2)} \cosh \alpha y + A_2^{(2)} \sinh \alpha y + A_3^{(2)} \cos \beta y + A_4^{(2)} \sin \beta y$$

8 integration constants have to be derived, consequently, the following boundary conditions have to be developed:

$$\begin{aligned} \varphi_1|_{y_1=0} = 0 & \quad \varphi_2|_{y_2=0} = 0 & \quad R_1^*|_{y_1=0} = 0 & \quad R_2^*|_{y_2=0} = 0 \\ w_1|_{y_1=b_1} = 0 & \quad w_2|_{y_2=-b_2} = 0 & \quad \varphi_1|_{y_1=b_1} = \varphi_2|_{y_2=-b_2} & \quad M_1|_{y_1=b_1} = M_2|_{y_2=-b_2} \end{aligned} \quad (40)$$

where w_i and φ_i are the kinematic conditions and they represent, respectively, the displacement and the rotation of a single plate. Instead, M_i and R_i^* are the static conditions and they represent the bending moment and the equivalent shear action, respectively. Their expressions in the elastic-plastic range are equal to:

$$M_i = -D_s \left[C_5 \frac{\partial^2 w}{\partial y^2} + (\nu + C_3 - 1) \frac{\partial^2 w}{\partial x^2} \right] \quad R_i^* = -D_s \left[C_5 \frac{\partial^3 w}{\partial y^3} + (C_3 + 1 - \nu) \frac{\partial^3 w}{\partial x^2 \partial y} \right] \quad (41)$$

It is important to underline that by applying the first four boundary conditions (rotations and equivalent shear equal to zero), it is obtained:

$$A_2^{(1)} = A_4^{(1)} = A_2^{(2)} = A_4^{(2)} = 0 \quad (42)$$

This result derived due to double symmetry. Instead, the remain boundary conditions lead to the following system of equations:

$$\begin{bmatrix} \cosh(\alpha_1 b_1) & \cos(\beta_1 b_1) & 0 & 0 \\ 0 & 0 & \cosh(\alpha_2 b_2) & \cos(\beta_2 b_2) \\ \alpha_1 \sinh(\alpha_1 b_1) & -\beta_1 \sin(\beta_1 b_1) & \alpha_2 \sinh(\alpha_2 b_2) & -\beta_2 \sin(\beta_2 b_2) \\ D_s^{(1)} \alpha_1^2 \cosh(\alpha_1 b_1) & -D_s^{(1)} \beta_1^2 \cos(\beta_1 b_1) & -D_s^{(2)} \alpha_2^2 \cosh(\alpha_2 b_2) & +D_s^{(2)} \beta_2^2 \cos(\beta_2 b_2) \end{bmatrix} \begin{Bmatrix} A_1^{(1)} \\ A_3^{(1)} \\ A_1^{(2)} \\ A_3^{(2)} \end{Bmatrix} = \begin{Bmatrix} 0 \\ 0 \\ 0 \\ 0 \end{Bmatrix} \quad (43)$$

Obviously, a trivial solution $\mathbf{A} = \mathbf{0}$ represents the unbuckled configuration. A nontrivial solution is provided when the axial load reaches a value such that the determinant of the coefficient matrix is equal to zero. This solution corresponds to occurrence of elastic-plastic buckling. It is important to underline that the solution of Eq.(43) can not be obtained in closed form, because the parameters α and β are dependent on the stress level and, consequently, on the value of the critical stress to be determined. For this reason, a numerical procedure has

been developed through the MATLAB software program[19]. Moreover, it is easy to recognize that the critical value of the stress in the elastic-plastic range $\sigma_{cr,p}$, corresponding to the bifurcation point of equilibrium, can be found for increasing values of the axial stress in the plate elements until the determinant of the coefficient matrix is equal to zero, as shown in Figure 4. More details of the previous procedure are reported also in [17] and [18].

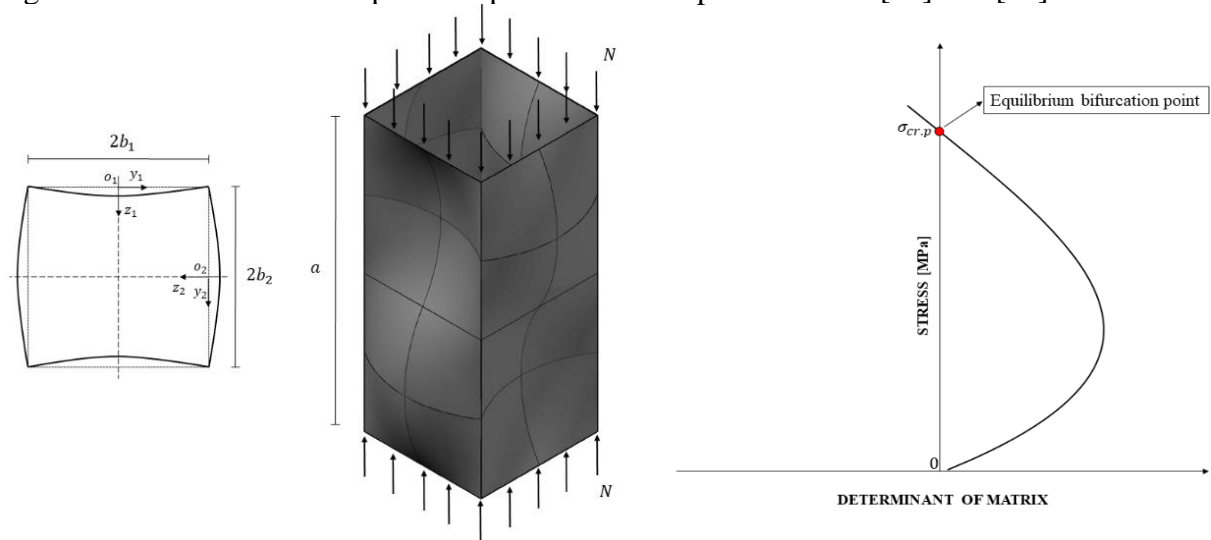


Figure 4. Geometric scheme of box section under compression (left). A generic trend between the determinant of matrix and the stress level in compression (right)

4. ANALYSIS AND RESULTS

In this section, an analysis performing on a generic box section by varying the width-to-thickness ratio and a comparison with experimental tests provided in the scientific literature are provided. The analysis has been carried out on the box-shaped members made of EN AW 6082-T6 aluminium alloy, characterized by the conventional yield strength equal to $f_{0.2} = 260$ MPa and the strain hardening coefficient equal to $n = 25$. It is important to underline that the material is modelled according to Ramberg-Osgood's law:

$$\varepsilon = \frac{\sigma}{E} + 0.002 \left(\frac{\sigma}{f_{0.2}} \right)^n \quad n = \frac{\ln(0.002/\varepsilon_{0,u})}{\ln\left(\frac{f_{0.2}}{f_u}\right)} \quad (44)$$

where $\varepsilon_{0,u}$ is the residual strain corresponding to the maximum stress f_u , and it is equal to $\varepsilon_{0,u} = \varepsilon_u - 0.002$. The analysis has been carried out for increasing the number buckling half-waves along the loading direction. The final value of the buckling stress will be the smallest among those computed. The result is depicted in Figure 5. It is easy to recognize that for the values of $b/t > 35$, the buckling effect occurs in the elastic region, while for values $b/t \leq 35$, the local buckling occurs in the post elastic range.

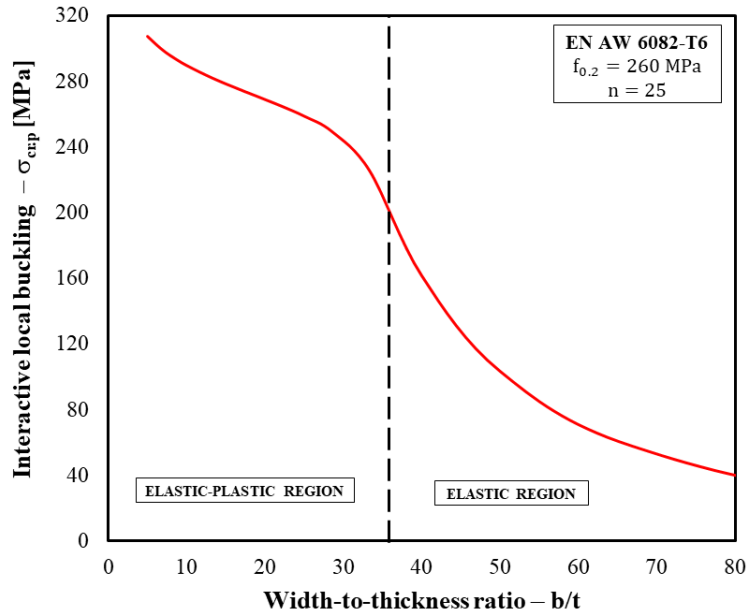


Figure 5. Trend between the width-to-thickness ratio and the interactive local buckling

In order to evaluate the accuracy of this procedure, a comparison with experimental stub column tests presented in the scientific literature. In particular, the experimental campaign performed by Su et al[20] at the University of Hong Kong and those carried out by Faella et al[21] at the University of Salerno have been considered in this work. The comparison has been provided in terms of the ultimate resistance and non-dimensional strain. Consequently, the theoretical buckling loads $N_{u,DTP}$, obtained by the deformation theory of plasticity procedure, are compared with the experimental results $N_{u,exp}$ as reported in Figure 6 (left). the comparison between the theoretic normalised strains $\bar{\epsilon}_{u,DTP}$, corresponding to $N_{u,DTP}$, and the experimental normalised strains $\bar{\epsilon}_{u,exp}$ is shown in Figure 6 (right). The normalization of the strain is performed by the value $\epsilon_0 = f_{0.2}/E$. The results of comparison are summarized in Table 1.

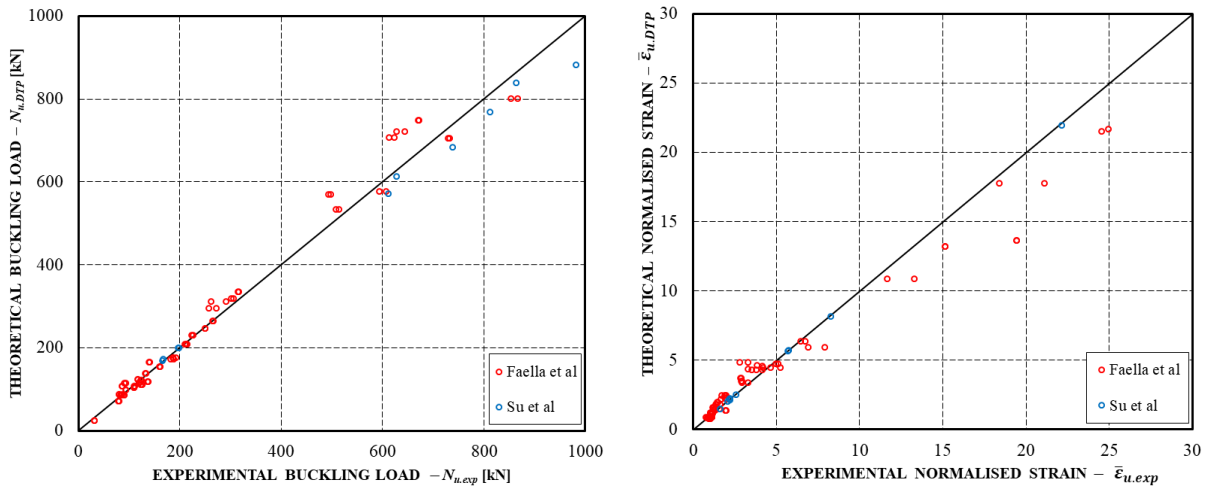


Figure 6. Comparison between the theoretic and experimental results in terms of the resistance (left) and the non-dimensional strain (right)

Table 1. Mean value and standard deviation of the $N_{u.DTP}/N_{u.exp}$ and $\bar{\epsilon}_{u.DTP}/\bar{\epsilon}_{u.exp}$ ratios

	Mean [μ]	Standard deviation [σ]
$N_{u.DTP}/N_{u.exp}$	1.03	0.09
$\bar{\epsilon}_{u.DTP}/\bar{\epsilon}_{u.exp}$	0.99	0.18

5. CONCLUSIONS

In this work, a theoretic procedure for evaluating the ultimate behaviour of aluminium members under uniform compression has been presented. Starting from the deformation theory of plasticity, the stability equation of a single plate under uniform compression is derived in the elastic-plastic region, considering the variability of Poisson ratio. Subsequently, the solution of the plate differential equation has been applied, by means of appropriate boundary conditions, to compute the interactive buckling occurring in the case of box sections.

The accuracy of fully theoretical approach has been evaluated by comparing the predicted buckling resistance and the corresponding strain with the results of available experimental tests. The obtained results have shown that the mean value of the ratio between the theoretical value of the ultimate resistance and the corresponding experimental value ($N_{u.DTP}/N_{u.exp}$) is equal to 1.03, with a standard deviation equal to 0.09. Instead, the mean value of the ratio between the theoretical value of non dimensional ultimate strain with those obtained by the experimental tests ($\bar{\epsilon}_{u.DTP}/\bar{\epsilon}_{u.exp}$) assumes value equal to 0.99 with a standard deviation equal to 0.18

Therefore, it can be concluded that the original theoretical contribution herein presented, is significant because it provides a comprehensive approach that evaluate with a good accuracy the local buckling resistance of aluminium members in compression by considering the variability of the Poisson ratio, the interaction between the plates composing the cross-section and the strain hardening behaviour of aluminium material.

REFERENCES

- [1] EN1999-1-1: Eurocode 9: Design of aluminium structures - Part 1-1: General structural rules, European Committee for Standardization, 2007.
- [2] V. Piluso, A. Pisapia, E. Nistri, R. Montuori, Ultimate resistance and rotation capacity of low yielding high hardening aluminium alloy beams under non-uniform bending. *Thin-Walled Structures*, Vol.135, pp. 123-136, 2019.
- [3] A. Pisapia, FEM calibration for aluminium I-beams under moment gradient. *International Conference on Numerical Analysis and Applied Mathematics 2018 (ICNAAM 2018)*, art. no. 260006, 2019.
- [4] A. Pisapia, V. Piluso, E. Nistri, R. Montuori, Ultimate behaviour of high yielding low hardening aluminium alloys I-beams. *Thin-Walled Structures*, Vol.146, Art.no.106463, 2020.
- [5] R. Montuori, E. Nistri, V. Piluso, A. Pisapia, The Influence of the Material Properties on the Ultimate Behaviour of Aluminium H-shaped Beams. *The Open Construction & Building Technology Journal*, Vol.15, pp. 176-188, 2021.

- [6] E. Nastro, V. Piluso, A. Pisapia, Experimental tests on SHS aluminium beams under non-uniform bending, *Engineering Structures*, Vol. 267, art. no. 114649, pp.1-16, 2022.
- [7] M.N. Su, B. Young, L. Gardner, The continuous strength method for the design of aluminium alloy structural elements. *Engineering Structures*, Vol.122, pp.338–348, 2016.
- [8] J.H. Zhu and B. Young, Design of aluminum alloy flexural members using direct strength method. *Journal of Structural Engineering*, Vol.135 (5), pp. 558-566, 2009.
- [9] E. Nastro, V. Piluso, A. Pisapia, Numerical application of effective thickness approach to box aluminium sections. *Journal of Composite Sciences*, Vol.5 (11), art. no. 291, 2021.
- [10] J. Blachut, G.D. Galletly, S. James, On the plastic buckling paradox for cylindrical shells. *Proc. Inst. Mech. Eng. Part C*, Vol. 210, pp. 477–488,1996.
- [11] R. Shamass, G. Alfano, F. Guarracino, An analytical insight into the buckling paradox for circular cylindrical shells under axial and lateral loading. *Math. Problems Eng*, Art.no.514267, 2015.
- [12] R. Shamass, Plastic Buckling Paradox: An Updated Review. *Frontiers in Built Environment*, Vol. 6, Art. no. 35, 2020.
- [13] E.Z. Stowell, A Unified Theory of Plastic Buckling of Columns and Plates. *National Advisory Committee for Aeronautics*, n. 1556, Washington D.C., 1948.
- [14] A.A. Ilyushin, The Elasto-Plastic Stability of Plates *National Advisory Committee for Aeronautics*, n. 1188 Washington D.C., 1946.
- [15] G. Gerard, S. Wildhorn, A Study of Poisson’s Ratio in the Yield Region. *National Advisory Committee for Aeronautics*, n. 2561 Washington D.C., 1952
- [16] R.M. Jones, Deformation Theory of Plasticity. *Bull Ridge Publishing*, Blacksburg, Virginia, 2009.
- [17] V. Piluso, A. Pisapia, Interactive Plastic Local Buckling of Box-shaped Aluminium Members under Uniform Compression. *Thin-Walled Structures*, Vol.164, Art. No. 107828, 2021.
- [18] V. Piluso, A. Pisapia, G. Rizzano, Local Buckling of Aluminium Channels under Uniform Compression: Theoretical Analysis and Experimental Tests. *Thin-Walled Structures*, Vol.179, Art. No. 109511, 2022.
- [19] MathWorks Inc. “MATLAB-High Performance Numeric Computation and Visualization Software. User’s Guide”, Natick: MA, USA, 1997.
- [20] M.N. Su, B. Young, L. Gardner, The continuous strength method for the design of aluminium alloy structural elements. *Engineering Structures*, Vol.122, pp.338–348, 2016.
- [21] C. Faella, F.M. Mazzolani, V. Piluso, G. Rizzano, Local buckling of aluminium members: testing and classification. *Journal of Structural Engineering*, Vol.126(3), pp.353–60, 2000.